2013 European Control Conference (ECC)
July 17-19, 2013, Zürich, Switzerland.

GAS Tightly Coupled LBL/USBL Position and Velocity Filter for Underwater Vehicles

Pedro Batista, Carlos Silvestre, and Paulo Oliveira

Abstract— **This paper presents a novel navigation filter for estimation of linear motion quantities based on a combined Long Baseline / Ultra Short Baseline (LBL/USBL) acoustic positioning system with application to underwater vehicles. The filtering algorithm does not resort to any algebraic inversion techniques and no linearizations are carried out whatsoever. In this way, the nonlinear sensor-based system dynamics are considered to their full extent and globally asymptotically stable (GAS) error dynamics are achieved. Finally, it is shown, under simulation environment, that the filter achieves very good performance in the presence of sensor noise.**

I. INTRODUCTION

The design of navigation systems is essential for the successful operation of autonomous vehicles. For aerial or ground vehicles the Global Positioning System (GPS) constitutes an important milestone. For underwater vehicles other solutions have been pursued due to the strong attenuation that the electromagnetic field suffers in water, in particular Long Baseline (LBL) and Short Baseline (SBL) acoustic positioning systems, see e.g. [1], [2], [3], [4], [5], [6], and references therein. Another commercially available solution is the GPS Intelligent Buoy (GIB) system, see [7]. Further work on the GIB underwater positioning system can be found in [8]. Position and linear velocity globally asymptotically stable (GAS) filters based on an Ultra-Short Baseline (USBL) positioning system were presented by the authors in [9], while the Extended Kalman Filter (EKF) is the workhorse of the solution presented in [10]. For interesting surveys on underwater navigation, the reader is referred to [11] and [12].

With a Long Baseline acoustic positioning system, an underwater vehicle has access to the distances to a set of known transponders, which are usually fixed in the mission scenario. With some mild assumptions on the LBL configuration, it is possible to determine the inertial position of the vehicle. With an Ultra-Short Baseline acoustic position system installed on-board the vehicle, in the so-called inverted configuration, see [13], the vehicle has access to the distance to a fixed transponder in the mission scenario and the time (or range) differences of arrival between each pair of receivers of the USBL array. From those measurements, and under some mild assumptions on the USBL array configuration, the position of the external landmark relative to the vehicle, and expressed in body-fixed coordinates, is readily available. Using spread spectrum techniques, see [14], it is possible to combine LBL and USBL acoustic positioning devices, which gives, in essence, both the distance between the vehicle and each of the external landmarks and the time (or range) differences of arrival between pairs of receivers, for each landmark. The goal of this paper is to design a filter for estimation of linear motion quantities (position and velocity) using all this information, in addition to attitude data, angular velocity, and relative velocity, as provided by an Attitude and Heading Reference System (AHRS) and a Doppler Velocity Log (DVL).

In previous work by the authors, see [15], a sensor-based solution was proposed for estimation of linear motion quantities with a LBL acoustic system, while in [13] a sensor-based solution was proposed with an USBL acoustic system. Central to the design, in both cases, was the derivation of augmented systems that, although still nonlinear, could be regarded as linear for observability and observer design purposes. With no linearizations whatsoever, that has resulted in exact observability analyses and the design of filtering solutions with globally asymptotically stable error dynamics. More recently, in [16], a novel solution was proposed that combines both a LBL and an USBL acoustic frameworks, yielding a complete navigation system that allows for the estimation of the inertial position, linear velocity, attitude and rate gyro bias. In contrast with the solutions proposed in [13] and [15], where the measurements are explicitly used by the filters, in the approach proposed in [16] the USBL/LBL is simply assumed to give the body-fixed positions of the external LBL landmarks, as well as the inertial position of the vehicle. These are obtained, in that framework, resorting to algebraic nonlinear operations that are carried out with the acoustic data that is provided by the LBL and USBL. As such, the actual measurements (travel times or, equivalently, the distances to the landmarks, and the time differences of arrival between acoustic receivers or, equivalently, the range differences of arrival,) are not explicitly used in the filtering process. This means, among others, that in poor LBL/USBL configurations, i.e., configurations with little redundancy, loss of one channel of the USBL or one of the LBL transponders, for instance, could prevent the computation of intermediate artificial measurements that are fed to the navigation filter.

The idea of this paper is, again, to combine both strategies, i.e., the USBL and the LBL acoustic positioning systems, to design an integrated LBL/USBL position and velocity filter. In contrast with the solution proposed in [16], the sensor measurements, i.e. ranges and range differences of arrival, are explicitly employed by the navigation filter. As such, loss

This work was partially supported by the FCT [PEst-OE/EEI/LA0009/2011] and by the EU Project TRIDENT (Contract No. 248497).

The authors are with the Institute for Systems and Robotics, Instituto Superior Técnico, Universidade Técnica de Lisboa, Av. Rovisco Pais, 1049-001 Lisboa, Portugal. Carlos Silvestre is also with the Department of Electrical and Computer Engineering, Faculty of Science and Technology of the University of Macau.

{pbatista,cjs,pjcro}@isr.ist.utl.pt

of one particular measurement does not invalidate the use of other measurements, which can potentially result in the increase of the performance of the overall system. Following previous work of the authors, the proposed methodology does not resort to any linearizations whatsoever and globally asymptotically stable error dynamics are achieved. This is, to the best of the authors' knowledge, the first contribution on the design of tightly coupled LBL/USBL navigation systems.

A. Notation

The symbol $\mathbf{0}$ denotes a matrix (or vector) of zeros, $\mathbf{I}$ the identity matrix, and $\mathbf{blkdiag}(\mathbf{A}_1, \ldots, \mathbf{A}_n)$ a block diagonal matrix, all assumed of appropriate dimensions. For $\mathbf{x}, \mathbf{y} \in \mathbb{R}^3$, the cross and inner products are represented by $\mathbf{x} \times \mathbf{y}$ and $\mathbf{x} \cdot \mathbf{y}$, respectively.

II. Problem Statement

Consider an underwater vehicle moving in a scenario where there is a set of fixed landmarks installed in a Long Baseline configuration and suppose that the vehicle is equipped with an Ultra Short Baseline acoustic positioning system, which measures not only the distance between the vehicle and each landmark but also the range differences of arrival between the acoustic receivers of the USBL, from each landmark, as depicted in Fig. 1. For further details on the USBL, the reader is referred to [13], [14], and references therein. Further assume that the vehicle is equipped with

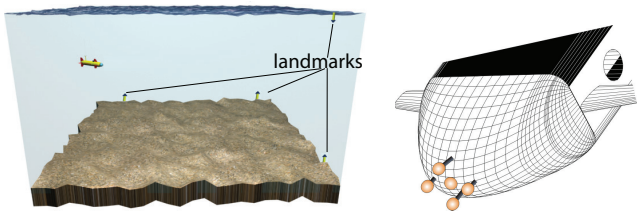

(a) AUV and LBL array (b) AUV with USBL array

Fig. 1. Mission Scenario

an Attitude and Heading Reference System, which provides both the angular velocity and the attitude of the vehicle, and a Doppler Velocity Log, which measures the velocity of the vehicle relative to the water. Finally, it is considered that the vehicle moves in the presence of a constant unknown ocean current. The problem considered in the paper is the design of a highly integrated sensor-based filter to estimate the inertial position of the vehicle and the ocean current velocity, with globally asymptotically stable error dynamics.

A. System dynamics

In order to set the problem framework, let $\{I\}$ denote a local inertial reference coordinate frame and $\{B\}$ a coordinate frame attached to the vehicle, commonly denominated as the body-fixed reference frame. The linear motion of the vehicle is described by

$$\dot{\mathbf{p}}(t) = \mathbf{R}(t)\mathbf{v}(t), \tag{1}$$

where $\mathbf{p}(t) \in \mathbb{R}^3$ denotes the inertial position of the vehicle, $\mathbf{v}(t) \in \mathbb{R}^3$ is the velocity of the vehicle relative to $\{I\}$ and expressed in body-fixed coordinates, and $\mathbf{R}(t) \in SO(3)$ is the rotation matrix from $\{B\}$ to $\{I\}$, which satisfies $\dot{\mathbf{R}}(t) = \mathbf{R}(t)\mathbf{S}(\boldsymbol{\omega}(t))$, where $\boldsymbol{\omega}(t) \in \mathbb{R}^3$ is the angular velocity of $\{B\}$, expressed in body-fixed coordinates, and $\mathbf{S}(\boldsymbol{\omega})$ is the skew-symmetric matrix such that $\mathbf{S}(\boldsymbol{\omega})\boldsymbol{x}$ is the cross product $\boldsymbol{\omega} \times \boldsymbol{x}$.

The AHRS provides the attitude of the vehicle, encoded in the rotation matrix $\mathbf{R}(t)$, and the angular velocity $\boldsymbol{\omega}(t)$, while the DVL provides the velocity of the vehicle relative to the water, expressed in body-fixed coordinates, denoted by $\mathbf{v}_r(t) \in \mathbb{R}^3$, such that

$$\mathbf{v}(t) = \mathbf{v}_r(t) + \mathbf{v}_c(t), \tag{2}$$

where $\mathbf{v}_c(t) \in \mathbb{R}^3$ is the ocean current velocity expressed in body-fixed coordinates. Finally, let $\mathbf{s}_i \in \mathbb{R}^3$, $i = 1, \ldots, N$, denote the inertial positions of the landmarks, and $\mathbf{a}_i \in \mathbb{R}^3$, $i = 1, \ldots, M$, the positions of the array of receivers of the USBL relative to the origin of $\{B\}$, expressed in body-fixed coordinates. Then, the range measurement between the i-th landmark and the j-th acoustic receiver of the USBL is given by

$$r_{i,j}(t) = \|\mathbf{s}_i - \mathbf{p}(t) - \mathbf{R}(t)\mathbf{a}_j\| \in \mathbb{R}. \tag{3}$$

Define $\mathbf{u}(t) := \mathbf{R}(t)\mathbf{v}_r(t)$ and let ${}^I\mathbf{v}_c(t) := \mathbf{R}(t)\mathbf{v}_c(t)$ denote the ocean current velocity expressed in inertial coordinates. Assuming it is constant, and combining (1), (2), and (3), yields the nonlinear system

$$\begin{cases} \dot{\mathbf{p}}(t) = {}^I\mathbf{v}_c(t) + \mathbf{u}(t) \\ {}^I\dot{\mathbf{v}}_c(t) = \mathbf{0}(t) \\ r_{1,1}(t) = \|\mathbf{s}_1 - \mathbf{p}(t) - \mathbf{R}(t)\mathbf{a}_1\| \\ \vdots \\ r_{N,M}(t) = \|\mathbf{s}_N - \mathbf{p}(t) - \mathbf{R}(t)\mathbf{a}_M\| \end{cases}. \tag{4}$$

The problem considered in the paper is the design of a filter for (4) assuming noisy measurements.

B. Long Baseline / Ultra Short Baseline configuration

Long Baseline acoustic configurations are one of the earliest methods employed for underwater navigation. These are characterized by the property that the distance between the transponders is long or similar to the distance between the vehicle and the transponders. This is in contrast with Ultra Short Baseline systems, where the distance between the transponder and the vehicle is much larger than the distance between receivers of the USBL system. In common is the fact that, under standard assumptions, both the inertial position of the vehicle (for the LBL) and the position of the landmarks with respect to the vehicle, expressed in body-fixed coordinates, (for the USBL, in the so-called inverted configuration) are uniquely determined. This happens with the following standard assumptions, which are considered in the remainder of the paper.

Assumption 1: The LBL acoustic positioning system includes at least 4 noncoplanar landmarks and the distance between the landmarks of the LBL is much larger than the distance between the receivers of the USBL acoustic positioning system.

Assumption 2: The USBL acoustic positioning system includes at least 4 noncoplanar receivers and the distance between the landmarks of the LBL is much larger than the distance between the receivers of the USBL acoustic positioning system.

III. Filter design

The design of a filter for the nonlinear system (4), considering also sensor noise, is detailed in this section. First, state and output augmentation are performed, in Section III-A, to attain a nominal system that, although nonlinear, can be regarded as linear for observability analysis and observer design purposes. Afterwards, the observability of that system is analyzed in Section III-B. Finally, in Section III-C, a Kalman filter for the resulting system, with globally asymptotically stable error dynamics, is briefly discussed.

A. State and output augmentation

In the recent past, a novel observer analysis and design technique has been proposed by the authors for navigation systems based on nonlinear range measurements, which consists basically in: i) include the range measurements in the system state; ii) identify the nonlinear terms of the dynamics of the range measurements as additional state variables; iii) define augmented outputs, when appropriate, to capture the structure of arrays of landmarks or receivers; and iv) work with the resulting nonlinear system, which can actually be regarded as linear time-varying, for observability analysis and observer design purposes. This approach has been successfully employed considering single measurements, see [17], LBL configurations, see [15], and USBL configurations, see [13], where different auxiliary sensors were considered, for example DVLs or triads of accelerometers. The design presented herein consists in the integration of both LBL/USBL measurements with this approach.

The time derivative of the range measurements (3) is given by

$$\dot{r}_{i,j}(t) = \tfrac{\mathbf{u}(t)+\mathbf{R}(t)\mathbf{S}(\boldsymbol{\omega}(t))\mathbf{a}_j}{r_{i,j}(t)} \cdot \mathbf{p}(t) + \tfrac{-\mathbf{s}_i+\mathbf{R}(t)\mathbf{a}_j}{r_{i,j}(t)} \cdot {}^I\mathbf{v}_c(t) + \tfrac{1}{r_{i,j}(t)}\mathbf{p}(t) \cdot {}^I\mathbf{v}_c(t) + u_{r_{i,j}}(t), \quad (5)$$

where

$$u_{r_{i,j}}(t) := \frac{\mathbf{u}^T(t)\mathbf{R}(t)\mathbf{a}_j - \mathbf{u}^T(t)\mathbf{s}_i - \mathbf{s}_i^T\mathbf{R}(t)\mathbf{S}\left(\boldsymbol{\omega}(t)\right)\mathbf{a}_j}{r_{i,j}(t)}.$$

Identifying the nonlinear term $\mathbf{p}(t) \cdot {}^I\mathbf{v}_c(t)$ in (5) with a new variable and taking its time derivative gives

$$\frac{d}{dt}\left[\mathbf{p}(t) \cdot {}^I\mathbf{v}_c(t)\right] = \mathbf{u}(t) \cdot {}^I\mathbf{v}_c(t) + \left\| {}^I\mathbf{v}_c(t)\right\|^2. \quad (6)$$

Finally, identifying the nonlinear term $\left\| {}^I\mathbf{v}_c(t)\right\|^2$ in (6) and taking its time derivative gives $\frac{d}{dt}\left[\left\| {}^I\mathbf{v}_c(t)\right\|^2\right] = 0$.

For the sake of clarity of presentation, let $\mathbf{x}_1(t) := \mathbf{p}(t)$, $\mathbf{x}_2(t) := {}^I\mathbf{v}_c(t)$, $x_{1,1}(t) := r_{1,1}(t), \ldots, x_{N,M}(t) := r_{N,M}(t)$, $x_3(t) := \mathbf{p}(t) \cdot {}^I\mathbf{v}_c(t)$, and $x_4(t) := \left\| {}^I\mathbf{v}_c(t)\right\|^2$, and define the augmented state vector as

$$\mathbf{x}(t) := \begin{bmatrix} \mathbf{x}_1(t) \\ \mathbf{x}_2(t) \\ x_{1,1}(t) \\ x_{1,2}(t) \\ \vdots \\ x_{N,M}(t) \\ x_3(t) \\ x_4(t) \end{bmatrix} \in \mathbb{R}^{3+3+NM+1+1}.$$

Then, the system dynamics can be written as

$$\dot{\mathbf{x}}(t) := \mathbf{A}(t)\mathbf{x}(t) + \mathbf{B}\mathbf{u}_a(t),$$

where $\mathbf{A}(t) \in \mathbb{R}^{(6+NM+2)\times(6+NM+2)}$,

$$\mathbf{A}(t) = \begin{bmatrix} \mathbf{0} & \mathbf{I} & \mathbf{0} & \mathbf{0} & \mathbf{0} \\ \mathbf{0} & \mathbf{0} & \mathbf{0} & \mathbf{0} & \mathbf{0} \\ \frac{\mathbf{u}^T(t)-\mathbf{a}_1^T\mathbf{S}(\boldsymbol{\omega}(t))\mathbf{R}^T(t)}{r_{1,1}(t)} & \frac{-\mathbf{s}_1^T+\mathbf{a}_1^T\mathbf{R}^T(t)}{r_{1,1}(t)} & \mathbf{0} & \frac{1}{r_{1,1}(t)} & 0 \\ \vdots & \vdots & \vdots & \vdots & \vdots \\ \frac{\mathbf{u}^T(t)-\mathbf{a}_M^T\mathbf{S}(\boldsymbol{\omega}(t))\mathbf{R}^T(t)}{r_{N,M}(t)} & \frac{-\mathbf{s}_N^T+\mathbf{a}_M^T\mathbf{R}^T(t)}{r_{N,M}(t)} & \mathbf{0} & \frac{1}{r_{N,M}(t)} & 0 \\ \mathbf{0} & \mathbf{u}^T(t) & \mathbf{0} & 0 & 1 \\ \mathbf{0} & \mathbf{0} & \mathbf{0} & 0 & 0 \end{bmatrix},$$

$$\mathbf{B} = \begin{bmatrix} \mathbf{I} & \mathbf{0} \\ \mathbf{0} & \mathbf{0} \\ \mathbf{0} & \mathbf{I} \\ \mathbf{0} & \mathbf{0} \\ \mathbf{0} & \mathbf{0} \end{bmatrix} \in \mathbb{R}^{(6+NM+2)\times(3+NM)},$$

and $\mathbf{u}_a(t) := \left[\mathbf{u}^T(t)\ u_{r_{1,1}}(t)\ \ldots\ u_{r_{N,M}}(t)\right]^T \in \mathbb{R}^{3+NM}$.

In order to define the output, notice that the states $x_{1,1}(t), \ldots, x_{N,M}(t)$ are measured. Note, however, that the range differences of arrival (RDOA) between pairs of receivers to the same landmark are measured more accurately with the USBL when compared to the distance between the landmark and any given receiver of the USBL. Selecting a reference sensor on the array, for instance receiver 1 for now, all the other ranges are easily reconstructed from the range measured at receiver 1 and the RDOA between receiver 1 and the other receivers. Hence, the first set of measurements that is considered is

$$\mathbf{y}_1(t) = \begin{bmatrix} r_{1,1}(t) \\ r_{1,1}(t) - r_{1,2}(t) \\ \vdots \\ r_{1,1}(t) - r_{1,M}(t) \\ \vdots \\ r_{N,1}(t) \\ \vdots \\ r_{N,1}(t) - r_{N,M}(t) \end{bmatrix} \in \mathbb{R}^{NM}. \quad (7)$$

However, if that was the only output to be considered, the LBL/USBL structure would not be encoded in the output. In order to capture the LBL/USBL structure, consider first the square of the range measurements, which is given by

$$r_{i,j}^2(t) = \|\mathbf{p}(t)\|^2 + \|\mathbf{s}_i\|^2 + \|\mathbf{a}_j\|^2 - 2\left[\mathbf{s}_i - \mathbf{R}(t)\mathbf{a}_j\right] \cdot \mathbf{p}(t) - 2\mathbf{s}_i^T\mathbf{R}(t)\mathbf{a}_j$$

for all $i = 1, \ldots, N$, $j = 1, \ldots, M$. Then,

$$r_{m,j}^2(t) - r_{n,j}^2(t) = \|\mathbf{s}_m\|^2 - \|\mathbf{s}_n\|^2 - 2\left(\mathbf{s}_m - \mathbf{s}_n\right) \cdot \left[\mathbf{p}(t) + \mathbf{R}(t)\mathbf{a}_j\right] \quad (8)$$

and

$$r_{i,m}^2(t) - r_{i,n}^2(t) = \|\mathbf{a}_m\|^2 - \|\mathbf{a}_n\|^2 - 2\left[\mathbf{R}(t)\left(\mathbf{a}_m - \mathbf{a}_n\right)\right] \cdot \left[\mathbf{s}_i - \mathbf{p}(t)\right]. \quad (9)$$

Breaking the differences of the squares, using $a^2 - b^2 = (a+b)(a-b)$, it follows from (8) and (9) that

$$2\tfrac{(\mathbf{s}_m-\mathbf{s}_n)^T}{r_{m,j}(t)+r_{n,j}(t)}\mathbf{x}_1(t) + x_{m,j}(t) - x_{n,j}(t) = \tfrac{\|\mathbf{s}_m\|^2-\|\mathbf{s}_n\|^2-2(\mathbf{s}_m-\mathbf{s}_n)^T\mathbf{R}(t)\mathbf{a}_j}{r_{m,j}(t)+r_{n,j}(t)} \quad (10)$$

and

$$-2\frac{(\mathbf{a}_m-\mathbf{a}_n)^T\mathbf{R}^T(t)}{r_{i,m}(t)+r_{i,n}(t)}\mathbf{x}_1(t)+x_{i,m}(t)-x_{i,n}(t)=\frac{\|\mathbf{a}_m\|^2-\|\mathbf{a}_n\|^2-2(\mathbf{a}_m-\mathbf{a}_n)^T\mathbf{R}^T(t)\mathbf{s}_i}{r_{i,m}(t)+r_{i,n}(t)}, \quad (11)$$

which capture the LBL/USBL structure. The augmented output can then be written as

$$\mathbf{y}(t)=\mathbf{C}(t)\mathbf{x}(t),$$

with $\mathbf{C}(t)\in\mathbb{R}^{\left(NM+M\,{}_2^NC+N\,{}_2^MC\right)\times(3+3+NM+1+1)}$,

$$\mathbf{C}(t)=\begin{bmatrix}\mathbf{0}&\mathbf{0}&\mathbf{C}_{13}&\mathbf{0}&\mathbf{0}\\ \mathbf{C}_{21}(t)&\mathbf{0}&\mathbf{C}_{23}&\mathbf{0}&\mathbf{0}\\ \mathbf{C}_{31}(t)&\mathbf{0}&\mathbf{C}_{33}&\mathbf{0}&\mathbf{0}\end{bmatrix},$$

where $\mathbf{C}_{13}:=\mathbf{blkdiag}\left(\mathbf{C}_{13}^0,\ldots,\mathbf{C}_{13}^0\right)\in\mathbb{R}^{\mathrm{NM}\times\mathrm{NM}}$, with

$$\mathbf{C}_{13}^0:=\begin{bmatrix}1&0&\ldots&\ldots&0\\ 1&-1&\ddots&&\vdots\\ 1&0&-1&\ddots&\vdots\\ \vdots&\vdots&\ddots&\ddots&0\\ 1&0&\ldots&0&-1\end{bmatrix}\in\mathbb{R}^{M\times M},$$

$$\mathbf{C}_{21}(t):=\begin{bmatrix}\mathbf{C}_{21}^1(t)\\ \vdots\\ \mathbf{C}_{21}^M(t)\end{bmatrix}\in\mathbb{R}^{\left(M\,{}_2^NC\right)\times3},$$

$$\mathbf{C}_{21}^i(t):=2\begin{bmatrix}\frac{(\mathbf{s}_1-\mathbf{s}_2)^T}{r_{1,i}(t)+r_{2,i}(t)}\\ \frac{(\mathbf{s}_1-\mathbf{s}_3)^T}{r_{1,i}(t)+r_{3,i}(t)}\\ \vdots\\ \frac{(\mathbf{s}_{N-1}-\mathbf{s}_N)^T}{r_{N-1,i}(t)+r_{N,i}(t)}\end{bmatrix}\in\mathbb{R}^{\,{}_2^NC\times3},$$

$$\mathbf{C}_{31}(t):=\begin{bmatrix}\mathbf{C}_{31}^1(t)\\ \vdots\\ \mathbf{C}_{31}^N(t)\end{bmatrix}\in\mathbb{R}^{\left(N\,{}_2^MC\right)\times3},$$

$$\mathbf{C}_{31}^i(t):=-2\begin{bmatrix}\frac{(\mathbf{a}_1-\mathbf{a}_2)^T\mathbf{R}^T(t)}{r_{i,1}(t)+r_{i,2}(t)}\\ \frac{(\mathbf{a}_1-\mathbf{a}_3)^T\mathbf{R}^T(t)}{r_{i,1}(t)+r_{i,3}(t)}\\ \vdots\\ \frac{(\mathbf{a}_{M-1}-\mathbf{a}_M)^T\mathbf{R}^T(t)}{r_{i,M-1}(t)+r_{i,M}(t)}\end{bmatrix}\in\mathbb{R}^{\,{}_2^MC\times3},$$

where ${}_2^NC=N(N-1)/2$ and ${}_2^MC=M(M-1)/2$ correspond to the numbers of 2-combinations of N and M elements, respectively, and $\mathbf{C}_{23}$ and $\mathbf{C}_{33}$ encode the differences of range measurements in (10) and (11), respectively, which are omitted as they are evident from the context. In short, $\mathbf{C}_{31}$ encodes (7), matrices $\mathbf{C}_{21}(t)$ and $\mathbf{C}_{23}$ encode (10) for all $j\in\{1,\ldots,M\}$ and $m,n\in\{1,\ldots,N\}$, with $n\neq m$, and matrices $\mathbf{C}_{31}(t)$ and $\mathbf{C}_{33}$ encode (11) for all $i\in\{1,\ldots,N\}$ and $m,n\in\{1,\ldots,M\}$, with $n\neq m$.

Considering the augmented system state and outputs, the final augmented system dynamics can be written as

$$\begin{cases}\dot{\mathbf{x}}(t)=\mathbf{A}(t)\mathbf{x}(t)+\mathbf{B}\mathbf{u}_a(t)\\ \mathbf{y}(t)=\mathbf{C}(t)\mathbf{x}(t)\end{cases}. \quad (12)$$

B. Observability analysis

The observability of the nonlinear system (12) and its relation with the original nonlinear system (4) is analyzed in this section.

Even though the system dynamics (12) resemble a linear time-varying system, the system is, in fact, nonlinear, as the system matrices depend both on the output and the input. However, this is not a problem for observability and observer design purposes and the results for linear time-varying systems still apply, see [17, Lemma 1]. Before presenting the main results, it is therefore convenient to compute the transition matrix associated with $\mathbf{A}(t)$ and the observability Gramian associated with the pair $(\mathbf{A}(t),\mathbf{C}(t))$. Long, tedious but straightforward computations allow to show that the transition matrix associated with $\mathbf{A}(t)$ is given by

$$\boldsymbol{\phi}(t,t_0)=\begin{bmatrix}\boldsymbol{\phi}_A(t,t_0)&\mathbf{0}&\mathbf{0}\\ \boldsymbol{\phi}_{BA}(t,t_0)&\mathbf{I}&\boldsymbol{\phi}_{BC}(t,t_0)\\ \boldsymbol{\phi}_{CA}(t,t_0)&\mathbf{0}&\boldsymbol{\phi}_{CC}(t,t_0)\end{bmatrix},$$

where

$$\boldsymbol{\phi}_A(t,t_0)=\begin{bmatrix}\mathbf{I}&(t-t_0)\mathbf{I}\\ \mathbf{0}&\mathbf{I}\end{bmatrix}\in\mathbb{R}^{6\times6},$$

$$\boldsymbol{\phi}_{BA}(t,t_0)=\begin{bmatrix}\boldsymbol{\phi}_{BA1}(t,t_0)&\boldsymbol{\phi}_{BA2}(t,t_0)\end{bmatrix}\in\mathbb{R}^{NM\times6},$$

$$\boldsymbol{\phi}_{BA1}(t,t_0)=\begin{bmatrix}\boldsymbol{\phi}_{BA1(1,1)}(t,t_0)\\ \vdots\\ \boldsymbol{\phi}_{BA1(N,M)}(t,t_0)\end{bmatrix}\in\mathbb{R}^{NM\times3},$$

$$\boldsymbol{\phi}_{BA1(i,j)}(t,t_0)=\int_{t_0}^{t}\frac{\mathbf{u}^T(\sigma)-\mathbf{a}_j^T\mathbf{S}(\boldsymbol{\omega}(\sigma))\mathbf{R}^T(\sigma)}{r_{i,j}(\sigma)}d\sigma,$$

$$\boldsymbol{\phi}_{BA2}(t,t_0)=\begin{bmatrix}\boldsymbol{\phi}_{BA2(1,1)}(t,t_0)\\ \vdots\\ \boldsymbol{\phi}_{BA2(N,M)}(t,t_0)\end{bmatrix}\in\mathbb{R}^{NM\times3},$$

$$\boldsymbol{\phi}_{BA2(i,j)}(t,t_0)=\int_{t_0}^{t}\frac{-\mathbf{s}_i^T+\mathbf{a}_j^T\mathbf{R}^T(\sigma_1)}{r_{i,j}(\sigma)}d\sigma_1+\int_{t_0}^{t}\frac{(\sigma-t_0)[\mathbf{u}(\sigma_1)+\mathbf{R}(\sigma_1)\mathbf{S}(\boldsymbol{\omega}(\sigma_1))\mathbf{a}_j]^T+\int_{t_0}^{\sigma_1}\mathbf{u}^T(\sigma_2)d\sigma_2}{r_{i,j}(\sigma)}d\sigma_1,$$

$$\boldsymbol{\phi}_{BC}(t,t_0)=\begin{bmatrix}\int_{t_0}^{t}\frac{1}{r_{1,1}(\sigma)}d\sigma&\int_{t_0}^{t}\frac{\sigma-t_0}{r_{1,1}(\sigma)}d\sigma\\ \vdots&\vdots\\ \int_{t_0}^{t}\frac{1}{r_{N,M}(\sigma)}d\sigma&\int_{t_0}^{t}\frac{\sigma-t_0}{r_{N,M}(\sigma)}d\sigma\end{bmatrix}\in\mathbb{R}^{NM\times2},$$

and $\boldsymbol{\phi}_{CA}(t,t_0)$ and $\boldsymbol{\phi}_{CC}(t,t_0)$ are omitted as they are not required in the sequel. The observability Gramian associated with the pair $(\mathbf{A}(t),\mathbf{C})$ is simply given by

$$\boldsymbol{\mathcal{W}}(t_0,t_f)=\int_{t_0}^{t_f}\boldsymbol{\phi}^T(t,t_0)\mathbf{C}^T(t)\mathbf{C}(t)\boldsymbol{\phi}(t,t_0)\,dt. \quad (13)$$

The following theorem addresses the observability of (12).

Theorem 1: Under Assumptions 1 or 2 (or both), the nonlinear system (12) is observable on $\mathcal{I}:=[t_0,t_f]$, $t_0<t_f$, in the sense that, given the system input $\{\mathbf{u}(t),t\in\mathcal{I}\}$ and the system output $\{\mathbf{y}(t),t\in\mathcal{I}\}$, the initial condition $\mathbf{x}(t_0)$ is uniquely determined.

Proof: The proof follows by contradiction. Suppose that the nonlinear system (12) is not observable in $\mathcal{I}$. Then, the observability Gramian $\boldsymbol{\mathcal{W}}(t_0,t_f)$ is not invertible, see

[17, Lemma 1], which means that there exists a unit vector $\mathbf{d} = \begin{bmatrix} \mathbf{d}_1^T & \mathbf{d}_2^T & \mathbf{d}_3^T & d_4 & d_5 \end{bmatrix}^T \in \mathbb{R}^{3+3+NM+1+1}$, with $\mathbf{d}_1 \in \mathbb{R}^3$, $\mathbf{d}_2 \in \mathbb{R}^3$, $\mathbf{d}_3 \in \mathbb{R}^{NM}$, and $d_4, d_5 \in \mathbb{R}$, such that

$$\mathbf{d}^T \boldsymbol{\mathcal{W}}(t_0, t)\, \mathbf{d} = 0 \tag{14}$$

for all $t \in \mathcal{I}$. Substituting (13) in (14) yields

$$\int_{t_0}^{t} \left\| \mathbf{C}(\tau)\, \boldsymbol{\phi}(\tau, t_0)\, \mathbf{d} \right\|^2 = 0 \tag{15}$$

for all $t \in \mathcal{I}$. Taking the time derivative of (15) gives

$$\left\| \mathbf{C}(t)\, \boldsymbol{\phi}(t, t_0)\, \mathbf{d} \right\|^2 = 0$$

for all $t \in \mathcal{I}$, which in turn implies that

$$\mathbf{C}(t)\, \boldsymbol{\phi}(t, t_0)\, \mathbf{d} = \mathbf{0} \tag{16}$$

for all $t \in \mathcal{I}$. With $t = t_0$ in (16) gives

$$\begin{cases} \mathbf{C}_{13}\mathbf{d}_3 = \mathbf{0} \\ \mathbf{C}_{21}(t_0)\, \mathbf{d}_1 + \mathbf{C}_{23}\mathbf{d}_3 = \mathbf{0} \\ \mathbf{C}_{31}(t_0)\, \mathbf{d}_1 + \mathbf{C}_{33}\mathbf{d}_3 = \mathbf{0} \end{cases}. \tag{17}$$

Notice first that $\mathbf{C}_{13}$ has full rank, which means that $\mathbf{d}_3 = \mathbf{0}$. On the other hand, under Assumption 1 matrix $\mathbf{C}_{21}(t_0)$ has full rank, while under Assumption 2 matrix $\mathbf{C}_{31}(t_0)$ has full rank. Hence, under the conditions of the theorem, is has been shown so far that the only solution of (17) is $\mathbf{d}_1 = \mathbf{0}$ and $\mathbf{d}_3 = \mathbf{0}$. Taking in the time derivative of (16) gives

$$\frac{d}{dt}\mathbf{C}(t)\, \boldsymbol{\phi}(t, t_0)\, \mathbf{d} = \mathbf{0}$$

for all $t \in \mathcal{I}$. In particular, for $t = t_0$, and considering $\mathbf{d}_1 = \mathbf{0}$ and $\mathbf{d}_3 = \mathbf{0}$, it is possible to write that

$$\left[-\mathbf{s}_i + \mathbf{R}(t_0)\, \mathbf{a}_j \right]^T \mathbf{d}_2 + d_4 = 0 \tag{18}$$

for all $i \in \{1, \ldots, N\}$ and $j \in \{1, \ldots, M\}$. Now, under Assumption 1 or 2 (or both), it is straightforward to show that the only solution of (18) is $\mathbf{d}_2 = \mathbf{0}$ and $d_4 = 0$. Finally, taking the second time derivative of (16), for $t = t_0$, and considering $\mathbf{d}_1 = \mathbf{d}_2 = \mathbf{0}$, $\mathbf{d}_3 = \mathbf{0}$, and $d_4 = 0$, it is straightforward to show that it must also be $d_5 = 0$. But this contradicts the hypothesis of existence of a unit vector $\mathbf{d}$ such that (14) holds. Hence, by contradicton, the observability Gramian $\boldsymbol{\mathcal{W}}(t_0, t_f)$ is invertible and hence the nonlinear system (12) is observable in the sense established in the theorem, see [17, Lemma 1]. ■

The fact that (12) is observable does not immediately entail that the nonlinear system (4) is observable nor that an observer for (12) is also an observer for (4), as there is nothing in the system dynamics (12) imposing the nonlinear algebraic relations that were at its own origin. Moreover, the range measurements as a nonlinear function of the state were also discarded. However, all that turns out to be true, as shown in the following theorem.

Theorem 2: Under Assumptions 1 or 2 (or both), the nonlinear system (4) is observable on $\mathcal{I} := [t_0, t_f]$, $t_0 < t_f$, in the sense that, given the system input $\mathbf{u}(t)$ and the system output $r_{1,1}(t), \ldots, r_{N,M}(t)$ for $t \in \mathcal{I}$, the initial condition $\mathbf{p}(t_0)$ and ${}^I\mathbf{v}_c(t_0)$ is uniquely determined. Moreover, the initial conditions of the augmented nonlinear system (12) match those of (4) and hence an observer with globally asymptotically stable error dynamics for (12) is also an observer for (4) with globally asymptotically stable error dynamics.

Proof: The proof is omitted due to space limitations. ■

C. Kalman filter

As a result of Theorem 2, a filtering solution for the nonlinear system (4) is simply obtained with the design of a Kalman filter for the augmented system (12), which can be regarded as LTV for this purpose as the output and input are available. The design is trivial and therefore it is omitted. Notice that the proposed solution is not an EKF, which would not offer GAS guarantees, and no approximate linearizations are carried out.

In order to guarantee that the Kalman filter has globally asymptotically stable error dynamics, stronger forms of observability are required, in particular uniform complete observability, see [18] and [19]. The pair $(\mathbf{A}(t), \mathbf{C}(t))$ can be easily shown to be uniformly completely observable following the same reasoning as in Theorem 1 but considering uniform bounds. The proof is omitted due to the lack of space.

IV. Simulation results

This section briefly presents some simulation results in order to give an idea of the performance achieved by the proposed solution. These are only preliminary results and they do not explore the full potential of the proposed solution, e.g. loss of measurements is not considered. Further results will be detailed in future work, including comparison with the EKF and Monte Carlo simulations.

In the simulations, the 3-D kinematic model for an underwater vehicle was employed. It is not necessary to consider the dynamics as the estimators are purely kinematic, hence the results apply to all underwater vehicles, regardless of the dynamics. The trajectory described by the vehicle is shown in Fig. 2. The LBL configuration is composed

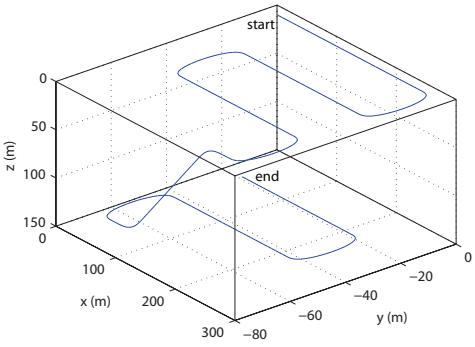

Fig. 2. Trajectory described by the vehicle

of 4 acoustic transponders and their inertial positions are $\mathbf{s}_1 = \begin{bmatrix} 1000 & 0 & 0 \end{bmatrix}(\mathrm{m})$, $\mathbf{s}_2 = \begin{bmatrix} 0 & 1000 & 0 \end{bmatrix}(\mathrm{m})$, $\mathbf{s}_3 = \begin{bmatrix} 1000 & 1000 & 0 \end{bmatrix}(\mathrm{m})$, $\mathbf{s}_4 = \begin{bmatrix} 0 & 0 & 100 \end{bmatrix}(\mathrm{m})$, while the positions of the USBL array receivers, in body-fixed coordinates, are $\mathbf{a}_1 = \begin{bmatrix} 0 & 0 & 0 \end{bmatrix}(\mathrm{m})$, $\mathbf{a}_2 = \begin{bmatrix} 0 & 0.3 & 0 \end{bmatrix}(\mathrm{m})$, $\mathbf{a}_3 = \begin{bmatrix} 0.20 & 0.15 & 0.15 \end{bmatrix}(\mathrm{m})$, $\mathbf{a}_4 = \begin{bmatrix} 0.20 & 0.15 & -0.15 \end{bmatrix}(\mathrm{m})$, hence both Assumptions 1 and 2 are satisfied.

Sensor noise was considered for all sensors. In particular, the LBL range measurements, the USBL range differences of arrival, and the DVL relative velocity readings are assumed to be corrupted by additive uncorrelated zero-mean white Gaussian noise, with standard deviations of $1\,\mathrm{m}$, $6 \times 10^{-3}\,\mathrm{m}$,

and $0.01\,\mathrm{m}$, respectively. The angular velocity measurements are also assumed to be perturbed by additive, zero mean, white Gaussian noise, with standard deviation of 0.05 °/s, and the attitude is provided by an AHRS with a mean angle error of 0.35 °, with the Euler angler-axis parameterization for the attitude error $\tilde{\mathbf{R}}(t) := \hat{\mathbf{R}}(t)\mathbf{R}(t)$, where $\hat{\mathbf{R}}(t)$ is the attitude estimate.

To tune the Kalman filter, the state disturbance intensity matrix was chosen as

$$\mathbf{blkdiag}\left(10^{-2}\mathbf{I},\, 10^{-4}\mathbf{I},\, 10^{-2},\, \ldots, 10^{-2},\, 10^{-2},\, 10^{-3}\right)$$

and the output noise intensity matrix as

$$\mathbf{blkdiag}\left(\mathbf{Q}_0, \mathbf{Q}_0, \mathbf{Q}_0, \mathbf{Q}_0, 1, \ldots, 1\right),$$

where $\mathbf{Q}_0 := \mathbf{blkdiag}\left(1,\, 0.6,\, 0.6,\, 0.6\right)$. The initial conditions were set to zero for all states.

The evolution of the position and velocity errors is depicted in Fig. 3. As it can be seen, the convergence rate of the filter is quite fast. While all the errors are very small, the most interesting fact is that the errors along the z-axis are much larger when compared with those along the x and y axes. This is directly related to the structure and baseline of the LBL array: the baseline along x and y is roughly 10 times the baseline aling z.

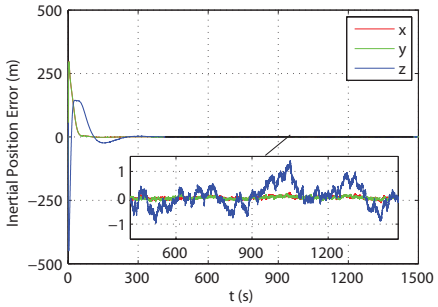

(a) Position error

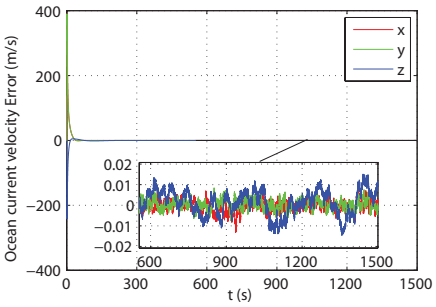

(b) Velocity error

Fig. 3. Evolution of the errors

V. Conclusions

This paper presented a novel approach for navigation of autonomous underwater vehicles that resorts to a combined LBL/USBL acoustic positioning device. The proposed filter for estimation of linear motion quantities is based on an augmented system that, although nonlinear, can be regarded as linear time-varying for observability analysis and observer design purposes. Hence, a Kalman filter was proposed, with globally asymptotically stable error dynamics, without any linearization whatsoever. In comparison with algebraic solutions for positioning, the present approach still works in case of failure of one or more range or range differences of arrival readings. Simulation results evidence fast convergence and performance. Future work will cover the comparison with existing techniques, in particular with the Extended Kalman Filter, the development of a multi-rate framework, and the analysis of the impact of errors of the AHRS.

References

[1] L. Whitcomb, D. Yoerger, and H. Singh, "Combined Doppler/LBL Based Navigation of Underwater Vehicles," in *Proceedings of the the 11th International Symposium on Unmanned Untethered Submersible Technology*, Durham, USA, Aug. 1999.

[2] J. Jouffroy and J. Opderbecke, "Underwater vehicle trajectory estimation using contracting PDE-based observers," in *Proceedings of the 2004 American Control Conference*, vol. 5, Boston, MA, USA, Jun-July 2004, pp. 4108–4113.

[3] J. Kinsey and L. Whitcomb, "Preliminary field experience with the DVLNAV integrated navigation system for manned and unmanned submersibles," in *Proceedings of the 1st IFAC workshop on guidance and control of underwater vehicles*, Newport, South Wales, UK, Apr. 2003, pp. 83–88.

[4] M. Larsen, "Autonomous navigation of underwater vehicles," Ph.D. dissertation, Department of Automation, Technical University of Denmark, 2001.

[5] ——, "Synthetic long baseline navigation of underwater vehicles," in *Proceedings of the 2000 MTS/IEEE Oceans*, vol. 3, Providence, RI, USA, Sep. 2000, pp. 2043–2050.

[6] J. Vaganay, J. Bellingham, and J. Leonard, "Comparison of fix computation and filtering for autonomous acoustic navigation," *International Journal of Systems Science*, vol. 29, no. 10, pp. 1111–1122, Oct. 1998.

[7] H. Thomas, "GIB buoys: an interface between space and depths of the oceans," in *Proceedings of the 1998 Workshop on Autonomous Underwater Vehicles*, Cambridge, MA, USA, Aug. 1998, pp. 181–184.

[8] A. Alcocer, P. Oliveira, and A. Pascoal, "Study and Implementation of an EKF GIB-based Underwater Positioning System," *Control Engineering Practice*, vol. 15, no. 6, pp. 689–701, Jun. 2007.

[9] P. Batista, C. Silvestre, and P. Oliveira, "Optimal position and velocity navigation filters for autonomous vehicles," *Automatica*, vol. 46, no. 4, pp. 767–774, Apr. 2010.

[10] M. Morgado, P. Oliveira, C. Silvestre, and J. Vasconcelos, "USBL/INS Tightly-Coupled Integration Technique for Underwater Vehicles," in *Proceedings of the 9th International Conference on Information Fusion*, Florence, Italy, Jul. 2006.

[11] J. Leonard, A. Bennett, C. Smith, and H. Feder, "Autonomous underwater vehicle navigation," MIT Marine Robotics Laboratory, Tech. Rep. Technical Memorandum 98-1, 1998.

[12] J. Kinsey, R. Eustice, and L. Whitcomb, "A Survey of Underwater Vehicle Navigation: Recent Advances and New Challenges," in *Proceedings of the 7th IFAC Conference on Manoeuvring and Control of Marine Craft*, Lisboa, Portugal, Sep. 2006.

[13] M. Morgado, P. Batista, P. Oliveira, and C. Silvestre, "Position USBL/DVLSensor-based Navigation Filter in the presence of Unknown Ocean Currents," *Automatica*, vol. 47, no. 12, pp. 2604–2614, Dec. 2011.

[14] M. Morgado, P. Oliveira, and C. Silvestre, "Design and experimental evaluation of an integrated USBL/INS system for AUVs," in *Proceedings of the 2010 IEEE International Conference on Robotics and Automation*, Anchorage, USA, May 2010, pp. 4264–4269.

[15] P. Batista, C. Silvestre, and P. Oliveira, "A Sensor-based Long Baseline Position and Velocity Navigation Filter for Underwater Vehicles," in *Proceedings of the 8th IFAC Symposium on Nonlinear Control Systems - NOLCOS 2010*, Bologna, Italy, Sep. 2010, pp. 302–307.

[16] ——, "GES Integrated LBL/USBL Navigation System for Underwater Vehicles," in *Proceedings of the 51st IEEE Conference on Decision and Control*, Maui, Hawaii, USA, Dec. 2011.

[17] ——, "Single Range Aided Navigation and Source Localization: observability and filter design," *Systems & Control Letters*, vol. 60, no. 8, pp. 665–673, Aug. 2011.

[18] S. Sastry and C. Desoer, "The robustness of controllability and observability of linear time-varying systems," *IEEE Transactions on Automatic Control*, vol. 27, no. 4, pp. 933–939, Aug. 1982.

[19] A. Jazwinski, *Stochastic Processes and Filtering Theory*. Academic Press, Inc., 1970.